Article

The Role of Magnetic Dipole—Dipole Coupling in Quantum Single-Molecule Toroics

Kieran Hymas [1] and **Alessandro Soncini** [1,2,*]

1   School of Chemistry, University of Melbourne, Parkville, VIC 3010, Australia; hymask@unimelb.edu.au
2   Dipartimento di Scienze Chimiche, Università degli Studi di Padova, Via Marzolo 1, 35131 Padova, Italy
*   Correspondence: alessandro.soncini@unipd.it

Abstract: For single-molecule toroics (SMTs) based on noncollinear Ising spins, intramolecular magnetic dipole–dipole coupling favours a head-to-tail vortex arrangement of the semi-classical magnetic moments associated with a toroidal ground state. However, to what extent does this effect survive beyond the semi-classical Ising limit? Here, we theoretically investigate the role of dipolar interactions in stabilising ground-state toroidal moments in quantum Heisenberg rings with and without on-site magnetic anisotropy. For the prototypical triangular SMT with strong on-site magnetic anisotropy, we illustrate that, together with noncollinear exchange, intramolecular magnetic dipole–dipole coupling serves to preserve ground-state toroidicity. In addition, we investigate the effect on quantum tunnelling of the toroidal moment in Kramers and non-Kramers systems. In the weak anisotropy limit, we find that, within some critical ion–ion distances, intramolecular magnetic dipole–dipole interactions, diagonalised over the entire Hilbert space of the quantum system, recover ground-state toroidicity in ferromagnetic and antiferromagnetic odd-membered rings with up to seven sites, and are further stabilised by Dzyaloshinskii–Moriya coupling.

Keywords: quantum Heisenberg ring; toroidal moment; single-molecule toroics; magnetic dipole–dipole interaction

1. Introduction

The existence of exotic electromagnetic multipoles, such as the toroidal moment, was first discussed in a pioneering work by Yanov Zel'dovich, where he proposed that, owing to the parity-violating effects of the electroweak force, Dirac particles ought to exhibit electromagnetic moments which were odd under both time- and parity-reversal operations [1]. Zel'dovich suggested that these moments might be realised in a classical electrodynamics setup in which poloidal electrical currents wrap around the tube of a torus, generating a circulating magnetic field throughout the solenoid and leading to a toroidal moment perpendicular to the ring. Subsequently, in 1997, Wood et al. successfully detected these moments in Caesium nuclei via parity non-conservation of $6\,s \rightarrow 7\,s$ atomic transitions in the presence of an inhomogeneous magnetic field [2]. The discovery of these exotic moments has led to a flurry of investigation, with some authors suggesting their use in negative refractive index metamaterials [3,4] and as a handle for the detection of dark matter [5]. The manifestation of toroidal moments in diamagnetic molecular species as a response to an applied inhomogeneous magnetic field has been reported [6–10]. In addition to other pioneering work in the analysis of magnetically induced current densities in molecules [11–14], Riccardo Zanasi and co-workers have provided useful insights into the toroidal response of diamagnetic molecules [15], even contributing recently a theory of dynamic molecular toroidisability, utilising optical electric fields [16].

The quantum toroidal moment arising from a molecular system comprised of N paramagnetic centres is quantified by the expectation value of the following toroidal moment operator:

$$\boldsymbol{\tau} = \sum_i \mathbf{r}_i \times \mathbf{m}_i \tag{1}$$

where $\mathbf{r}_i$ is the position vector of the ith paramagnetic ion and $\mathbf{m}_i$ is its magnetic moment (for ions with a pure spin ground multiplet, modelled with the local spin operators $\mathbf{S}_i$, the local magnetic moments are $\mathbf{m}_i = g\mu_B\mathbf{S}_i$ with μ_B as the Bohr magneton and g as the electron g-value). From a semi-classical perspective, and in the absence of orbital currents, the toroidal moment can be visualised as a collection of magnetic moments arranged tangentially to a molecular ring in a vortex configuration [9,17,18]. Thus, paramagnetic cycles with strong on-site magnetic anisotropy oriented in the plane of the ring represent the most promising candidates for single-molecule toroics.

In fact, since the first prediction [19], preparation [20] and observation [21] of ground-state toroidal moments in magnetically anisotropic rings with nearest-neighbour exchange connectivity, the syntheses of three- [22–25], four- [26–28] and six-membered [29–31] rings comprised of strongly magnetically anisotropic Ln^{3+} ions have been reported in the literature, with theoretical models supporting the existence of ground-state toroidal moments in each case. Efforts to maximise the molecular toroidal moment have also been undertaken in an attempt to realise materials displaying toroidally ordered phases, either by coupling Ln_3 triangular subunits intramolecularly with $3d$ metal ions [32–35] or by grafting them together in planar configurations [36–38].

Despite the ubiquity of semi-classical Ising spin models for the characterisation of single-molecule toroics, it was demonstrated in one of the early works [19] that quantum spin fluctuations induced by the transversal spin components of a Heisenberg exchange interaction can disrupt the formation of toroidal ground states (with a non-intuitive geometric dependence) by introducing a tunnel splitting between the otherwise degenerate semi-classical spin vortex ground states of the paramagnetic ring. Such a tunnelling ground state (i.e., a linear superposition of toroidal states) sets the stage for quantum computation based on toroidal qubits given appropriate quantum gating operations could be performed on a timescale shorter than spin–lattice and spin–spin dephasing processes [39]. Quantum effects are also pertinent for the realisation of toroidally polarisable ground states for quantum information technologies based on spin-frustrated $3d$ metal triangles with weak or vanishing on-site magnetic anisotropy [40,41]. The coherent control of chiral (not toroidal) quantum states in molecular triangles through localised electric field pulses, by means of spin–electric coupling, has been previously suggested [18,42–45] and was recently demonstrated for a Cu_3 triangle [46]. Since the quantum toroidal states of the spin frustrated ring may be prepared from the chiral states via an $SU(2)$ basis rotation, it may then be feasible to address the toroidal states of a $3d$ metal triangle, in second order, via the coherent manipulation of its chiral states. Unfortunately, for $N > 3$-odd-membered rings, spin frustration is a necessary but insufficient condition to observe ground-state toroidal moments. When only an antiferromagnetic isotropic exchange interaction between nearest neighbours in the ring is considered, toroidal states emerge only in excited spin multiplets for $N = 5$-, 7- and 9-membered rings (vide infra). It has previously been suggested that these states can be stabilised by next-nearest-neighbour exchange interactions, albeit for rather stringent connectivities, which may be difficult to realise synthetically [47].

Intramolecular magnetic dipole–dipole interactions are regularly considered in the theoretical characterisation of semi-classical SMTs based on strongly magnetically anisotropic $4f$ ions, in which case they favour head-to-tail vortex configurations of spin dipoles in the ring, hence the stabilising molecular toroidal states. In this work, we investigate the role of magnetic dipole–dipole interactions in *quantum* single-molecule toroics in the strong and weak anisotropy regimes, where the full noncollinear Heisenberg exchange can, in principle, remove ground-state toroidicity altogether. The extent to which intra-ring dipole coupling may preserve ground-state toroidicity will be discussed in both limits of magnetic

anisotropy, and hence can guide the synthesis of future quantum SMTs for future quantum information applications.

2. Quantum Heisenberg Triangle with Strong On-Site Magnetic Anisotropy

To investigate the dependence of magnetic axis canting angle on the ground-state toroidal moment with and without the inclusion of magnetic dipole–dipole coupling, we consider a ring comprised of three paramagnetic ions located in the *xy*-plane at $\mathbf{r}_i = \left(R \cos\left(\frac{2\pi(i-1)}{3} \right), R \sin\left(\frac{2\pi(i-1)}{3} \right), 0 \right)$. Trivalent dysprosium atoms have, as of late, been the ions of choice for the synthesis of SMTs, owing to their large magnetic moment and often thermally well-isolated ground-state $m_J = \pm 15/2$ doublet. In recent theoretical models of such systems [21,28,33], these ions are treated as pseudo-spin 1/2 semi-classical entities with strongly axial g-tensors. As a first step to recovering quantum effects in the prototypical SMT triangle, we choose an on-site $S = 3/2$ ion as the simplest example of a Kramers system displaying on-site magnetic anisotropy; our model is readily extended to larger spin lengths. The on-site magnetic anisotropy and nearest-neighbour Heisenberg exchange connectivity of the ring is well described by the following Hamiltonian model [19]:

$$H = -D \sum_i S_{i,z}^2 - J_{\text{ex}} \sum_{\langle ij \rangle} \mathbf{S}_i \cdot \mathbf{S}_j \tag{2}$$

where the *i*th spin operator $\mathbf{S}_i$ is quantised along the local noncollinear magnetic axis specified by $\mathbf{n}_i = \left(\sin\left(\frac{2\pi(i-1)}{3} \right) \sin(\theta), -\cos\left(\frac{2\pi(i-1)}{3} \right) \sin(\theta), \cos(\theta) \right)$, with θ as the uniform canting angle of the axes (see Figure 1a). In Equation (2), $D > 0$ is the magnitude of an easy-axis magnetic anisotropy and J_{ex} is the Heisenberg exchange coupling constant between nearest neighbours $\langle ij \rangle$ in the triangle. Notably, the microscopic origins of on-site, axial magnetic anisotropy for paramagnetic rings constituted by transition metal ions or by lanthanide ions is rather different. Magnetic anisotropy, in the former case, generally arises from a partial recovery of orbital angular momentum in the pure spin ground multiplet, $^{2S+1}\Gamma_0$, of each ion, through spin–orbit coupling effects in second-order perturbation theory, thus leading to a zero-field splitting of the otherwise $2S + 1$-degenerate M_S levels of each ion in the ring. In the latter case, however, where strong spin–orbit coupling necessitates the use of the total angular momentum operator, $\mathbf{J} = \mathbf{L} + \mathbf{S}$, the comparatively weak ligand field of each ion lifts the $2J + 1$ degeneracies of each spin–orbit multiplet $^{2S+1}L_J$ in first-order perturbation theory via the crystal field Hamiltonian $H_{\text{CF}} = \sum_{qk} B_k^q \mathcal{O}_k^q$, where $\mathcal{O}_k^q$ are even-rank Stevens' operators [48] with $q = 2, 4$ and 6, $-q \leq k \leq q$ and real coefficients B_k^q. If one had in mind a particular molecular ring, then complete active-space, self-consistent field (CASSCF) calculations, beginning from a microscopic Hamiltonian, might be employed for each paramagnetic ion in the ring (with all others substituted with their diamagnetic analogues), to uncover the direction and magnitude of on-site magnetic anisotropy [33,35]. Furthermore, intramolecular exchange coupling can be approximated using the broken symmetry density functional theory approach pioneered by Noodleman [49] and which is often utilised in the study of molecular wheels composed of paramagnetic ions [50,51]. While the model Hamiltonian presented in Equation (2) clearly represents an approximation to the full electrostatic Hamiltonian for the ring, it nonetheless embodies the minimal physical ingredients required to capture a non-intuitive geometric dependence of the strongly axial on-site magnetic anisotropy on the toroidal ground-state properties of the prototypical triangular SMT motif.
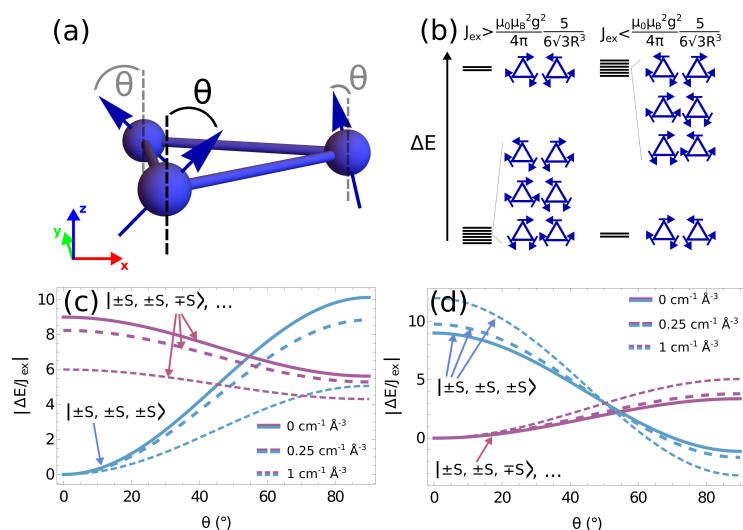
Figure 1. (**a**) Schematic depiction of the molecular triangle with on-site magnetic anisotropy axes (blue arrows) arranged tangentially about the vertices of the triangle and canted by an angle θ from $\hat{\mathbf{z}}$. (**b**) Ground and first excited exchange multiplets of the semi-classical Ising states of the triangle with idealised in-plane magnetic anisotropy $\theta = 90°$. (**c**,**d**) Energy as a function of canting angle θ of the lowest lying Ising exchange manifolds in the semi-classical on-site spin $S = 3/2$ molecular triangle for ratios of $|J_{\text{ex}}|/R^3 = 0$ cm^{-1} Å^{-1} (solid), 0.25 cm^{-1} Å^{-1} (dashed) and 1 cm^{-1} Å^{-1} (fine dashed) for (**c**) ferromagnetic and (**d**) antiferromagnetic exchange coupling J_{ex}.

In addition to the Heisenberg exchange Hamiltonian, with strong on-site magnetic anisotropy, as presented above, we extend the model of Ref. [19] by including also magnetic dipole–dipole interactions between paramagnetic ions in the ring using the following well-known dipolar Hamiltonian [52]:

$$H_{\text{dip}} = \frac{\mu_0 \mu_B^2 g^2}{4\pi} \sum_{ij} \left(\frac{\mathbf{S}_i \cdot \mathbf{S}_j}{\left|\mathbf{R}_{ij}\right|^3} - 3 \frac{\left(\mathbf{S}_i \cdot \mathbf{R}_{ij}\right)\left(\mathbf{S}_j \cdot \mathbf{R}_{ij}\right)}{\left|\mathbf{R}_{ij}\right|^5} \right) \tag{3}$$

where μ_0 is the permeability of free space and $\mathbf{R}_{ij} = \mathbf{r}_i - \mathbf{r}_j$ is the displacement vector between sites i and j. Typically in paramagnetic triangles with strong on-site anisotropy, the displacement vectors are on the order of $\left|\mathbf{R}_{ij}\right| \sim$ 3–4 Å [20,22,32,33], so that the strength of dipole–dipole interactions in the ring is of the order $E_{\text{dip}} \sim \mu_0 \mu_B^2 g^2/4\pi R^3 = 0.2$ cm^{-1} (note that, for paramagnetic ions with unquenched orbital angular momentum, $g\mu_B$ should be replaced with $\bar{\mu}$, the magnetic moment of the ion, e.g., $\bar{\mu} \approx 10\,\mu_B$ for Dy^{3+}, leading to a much stronger intramolecular dipole interaction). In contrast to previous theoretical models, here we consider the exact eigenstates of Equation (2), which include quantum fluctuations between Ising configurations, and which are clearly further influenced by the transverse components of the dipolar-spin Hamiltonian Equation (3).

2.1. The Semi-Classical Ising Picture

Before proceeding to the fully quantum spin ring, we first consider the semi-classical limit of the triangular SMT, formally obtained by letting $D \to \infty$ in Equation (3). In this limit, the ground multiplet of the triangle consists of states with maximal spin projections $m_i = \pm S$ along the noncollinear magnetic axes of the triangle, which are then split into sets of degenerate levels by the semi-classical exchange and magnetic dipole interactions. The energy of each state $|\mathbf{m}\rangle = |m_1, m_2, m_3\rangle$ (up to a common additive constant from the zero-field splitting) is

$$E_{\mathbf{m}} = \left[-J_{\text{ex}} \left(\cos^2\theta - \frac{1}{2}\sin^2\theta \right) + \frac{\mu_0 \mu_B^2 g^2}{4\pi} \frac{\left(\cos^2\theta - \frac{5}{4}\sin^2\theta\right)}{3\sqrt{3}R^3} \right] \sum_i m_i m_{i+1} \tag{4}$$

where a non-trivial angular dependence of the magnetic axes already emerges in both the exchange and dipole coupling parts. In Figure 1b, we illustrate the splitting of the ground-state multiplet for an idealised SMT with completely in-plane magnetic anisotropy. When the exchange coupling is ferromagnetic and overcomes magnetic dipole–dipole coupling, the resultant ground state is sixfold degenerate and consists of configurations with a net magnetic moment in the plane of the triangle [53]. These states are referred to as exchange-frustrated states, and do not support a toroidal moment. On the other hand, when J_{ex} is weaker than magnetic dipole coupling or J_{ex} is antiferromagnetic, a toroidal doublet characterised by the vortex arrangement of the magnetic moments about the triangle is stabilised. In Figure 1c,d, we explore the energetic stabilisation of these two manifolds for a molecular triangle with on-site spin $S = 3/2$ as a function of canting angle θ when J_{ex} is ferromagnetic or antiferromagnetic. Notably, for the strengths of dipole–dipole coupling explored here, a level crossing between each manifold always occurs as a function of canting angle. From Equation (4), the angle at which the level crossing occurs is $\theta_0 = \arctan\left(\sqrt{-\alpha/\beta}\right)$, where $\alpha = -J_{ex} + \frac{\mu_0 \mu_B^2 g^2}{4\pi} \frac{1}{3\sqrt{3}R^3}$ and $\beta = \frac{J_{ex}}{2} - \frac{\mu_0 \mu_B^2 g^2}{4\pi} \frac{5}{12\sqrt{3}R^3}$. Notably, θ_0 depends upon the microscopic electronic parameters of the ring as well as its inherent geometry. For ferromagnetic coupling $J_{ex} > 0$, Figure 1c illustrates that the doubly degenerate toroidal manifold is stabilised between $0° < \theta \le \theta_0$ with magnetic dipole–dipole coupling moving the level crossing to larger θ. For antiferromagnetic coupling, the semi-classical toroidal states are stabilised between $\theta_0 \le \theta \le 90°$ where dipole–dipole coupling acts to reduce θ_0.

2.2. The Role of Magnetic Dipole–Dipole Coupling in Quantum SMTs

Surpassing the semi-classical Ising approximation activates all non-axial terms in Equations (2) and (3). To see the effect of these quantum fluctuations on the ground-state toroidal moment of the on-site $S = 3/2$ SMT triangle, we diagonalise the lowest degenerate manifold of energy eigenstates obtained from Equations (2) and (3) on the z projection of the toroidal moment operator given in Equation (1) and plot the absolute magnitude of the resultant eigenvalues (the magnitude of the toroidal moment) against the uniform magnetic axis canting angle θ in Figure 2a,b. In correspondence with the semi-classical Ising picture, for the ferromagnetic-exchange-coupled triangle, we observe a linearly increasing toroidal moment with increasing canting angle θ that abruptly falls to zero when the semi-classical vortex spin states become excited states of the system (see Figure 1c). When the Heisenberg exchange coupling is antiferromagnetic, not only does the system exhibit a non-zero toroidal moment for $\theta > \theta_0$ where the Ising-like vortex spin states form the ground state of the semi-classical system, but also, a non-zero toroidal moment appears in the canting angle domain $0° < \theta \le 30°$. When $0° < \theta \le 30°$, the sixfold *quasi*-degenerate exchange frustrated states may be prepared in linear combinations to form weakly toroidal and non-toroidal states (a phenomenon that will be discussed at length in Section 3 of this manuscript). The formation of this linear combination is only possible when *quasi*-degeneracy of all six exchange frustrated states of the triangle is retained and, due to their energetic splitting into three isolated doublets with increased canting angle, persists only up until $\theta \approx 30°$.

The effect of magnetic dipole–dipole coupling in both cases of exchange coupling is to extend the domain of magnetic axis canting angle in which the triangle displays a non-zero toroidal moment. Setting aside for now the non-zero toroidal moment observed for the antiferromagnetically coupled triangle with $\theta < 50°$, the extension of a non-zero toroidal moment to higher (lower) canting angles for ferromagnetic (antiferromagnetic) exchange coupling corresponds directly to the shifting of θ_0 by the magnetic dipole–dipole interaction illustrated for the semi-classical Ising model in Figure 1c,d. Notably, we observe that diagonalising the intramolecular magnetic dipole–dipole coupling Hamiltonian over the entire Hilbert space of the $S = 3/2$ triangle (in addition to the magnetic anisotropy and exchange terms) leads to a preservation of a weak toroidal moment expectation value up to $\theta \approx 50°$, shown by the blue dashed curves in Figure 2d. Magnetic dipole–dipole

coupling works here to maintain the sixfold *quasi*-degeneracy of the exchange frustrated spin states, such that their linear combination into toroidally polarised states is possible for canting angles $\theta > 30°$. This effect will be discussed further later in the manuscript when we consider the vanishing on-site magnetic anisotropy limit of SMTs.
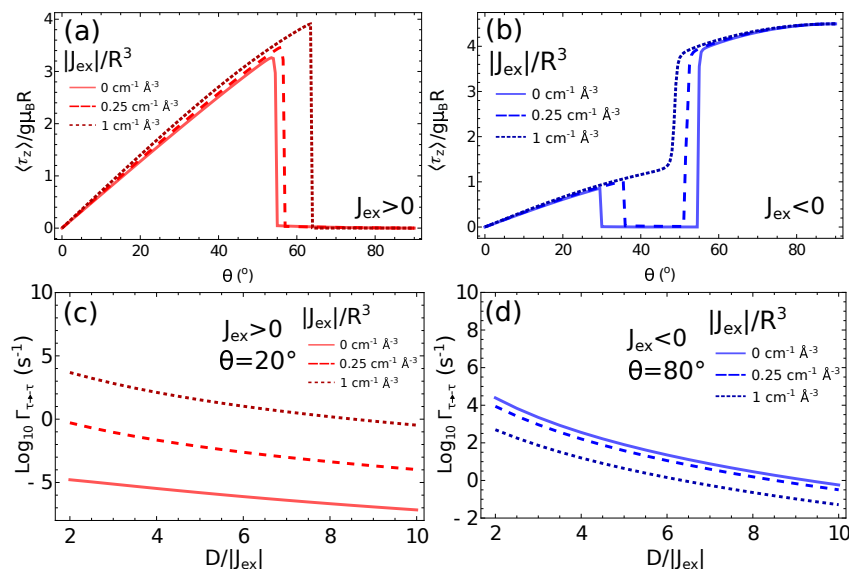

Figure 2. (**a**,**b**) Expectation value of the toroidal moment as a function of canting angle θ for the on-site $S = 3/2$ molecular triangle with a fixed ratio of $|D/J_{ex}| = 10$ and (**a**) ferromagnetic and (**b**) antiferromagnetic exchange coupling. (**c**,**d**) Base 10 logarithm of the tunnelling rate between toroidal states in the molecular triangle induced by a stray magnetic dipole. (**c**) Tunnelling rates in the ferromagnetically coupled triangle with magnetic axis canting angle $\theta = 20°$. (**d**) Tunnelling rates in the antiferromagnetically coupled triangle with magnetic axis canting angle $\theta = 80°$. The effect of intramolecular magnetic dipole–dipole coupling between paramagnetic ions in the SMT on the stray-dipole-assisted tunnelling rate is highlighted by vanishing (solid line), intermediate (dashed line) and strong (fine dashed line) intramolecular dipole–dipole coupling.

It is particularly interesting (and relevant for the development of SMT qubits) to investigate the effect of intramolecular magnetic dipole–dipole coupling on the tunnelling of the toroidal moment. For a Kramers system, such as the $S = 3/2$ triangle, the tunnelling of the toroidal moment occurs via coupling to stray dipolar fields, $\mathbf{B}_{stray}$, in the vicinity of the paramagnetic centres. Provided that these stray fields are weak with respect to intramolecular exchange and magnetic dipole–dipole coupling, transitions between toroidal ground states can be calculated in first-order perturbation theory using the following Fermi golden rule:

$$\Gamma_{\pm\tau \to \mp\tau} = \frac{2\pi\rho}{\hbar} \left| \langle \mp\tau | g\mu_B \sum_{i=1}^{3} \mathbf{S}_i \cdot \mathbf{B}_{stray} | \pm\tau \rangle \right|^2 \tag{5}$$

where $|\pm\tau\rangle$ are toroidal states comprised of appropriate linear combinations of the Ising-type basis states $|m_1, m_2, m_3\rangle$, which are brought about by the activation of all non-axial terms in Equations (2) and (3); ρ is the density of states taken here to be unity; and $\mathbf{B}_{stray} = \lambda\hat{\mathbf{z}}/r^3$ is a stray magnetic field originating from a nearby dipole located at $\mathbf{r}$. To approximate the strength of this stray field, we consider a nearby dipole, $|\mathbf{m}| \sim 10\mu_B$, so that $\lambda = \mu_0|\mathbf{m}|/4\pi \approx 9.274$ T Å^3. For typical intermolecular distances $r \sim 8$ Å [20,54], the magnitude of nearby stray dipolar fields is on the order of $|\mathbf{B}_{stray}| \sim 15$ mT. This analysis indicates that the Fermi golden rule approach is well suited for calculating toroidal moment tunnelling rates induced by stray dipolar fields, since the magnitude of such fields is, at best, an order of magnitude smaller than typical intramolecular exchange and magnetic dipole–dipole coupling.

Utilising the above approximation, in Figure 2c,d, we plot the Fermi golden rule tunnelling rate of the molecular toroidal moment assisted by the stray dipolar field $\mathbf{B}_{\text{stray}}$ for representative geometries of the $S = 3/2$ triangle with ferromagnetic and antiferromagnetic exchange coupling, respectively. Interestingly, in the case of ferromagnetic coupling, the rate of stray-field-induced tunnelling of the ground-state toroidal moment is increased when stronger intramolecular magnetic dipole–dipole coupling is experienced between the paramagnetic ions of the ring. For an antiferromagnetically coupled ring, stronger intramolecular magnetic dipole–dipole coupling serves to protect against stray-field-induced tunnelling of the toroidal moment by reducing the rate of tunnelling between the toroidal states; while only representative canting angles of $\theta = 20°$ and $\theta = 80°$ are shown here, this trend persists for all other canting angles for which toroidal ground states can be prepared.

2.3. Tunnelling of the ground-state Toroidal Moment in a Non-Kramers System

As was previously demonstrated for an $N = 6$ molecular wheel with on-site spin $S = 1$ and noncollinear magnetic axes [19], the transversal components of the noncollinear exchange coupling (and here the magnetic dipole–dipole coupling), proportional to the ladder operators $S_{i,\pm} S_{i+1,\pm}$, can connect the semi-classical toroidal ground states in $N \times S^{\text{th}}$-order perturbation theory, leading to a tunnelling ground state which is a linear combination of both semi-classical vortex configurations of the ring $|\pm S, \ldots, \pm S\rangle$. Consequently, a large tunnel splitting caused by the transversal couplings erases the ground-state toroidal moment in a non-Kramers triangle (and also in larger rings). The realisation of a ground-state superposition of the toroidal moment nevertheless represents an important first step towards the development of quantum computation based on toroidal qubits.

To re-illustrate the findings of Ref. [19], now, however, for the on-site $S = 1$ molecular triangle, we numerically diagonalise Equation (2) and calculate the splitting Δ between ground and first excited states in the triangle (this gap corresponds to the tunnel splitting between vortex configurations of the semi-classical Ising states). In Figure 3a,b, we plot the ground-state toroidal moment of the triangle obtained by diagonalising the *quasi*-degenerate ground manifold of energy eigenstates (obtained from Equation (2)) on the z-projection of the toroidal moment operator in Equation (1). With both intermediate $|D/J_{\text{ex}}| = 5$ and strong on-site magnetic anisotropy $|D/J_{\text{ex}}| = 10$, a ground-state toroidal moment is observed for $J_{\text{ex}} > 0$ between $0 < \theta \lesssim 50°$, where the tunnel splitting between the ground states Δ, is vanishingly small. Since $\Delta < 10^{-2}$ cm^{-1} in this region, the *quasi*-degenerate ground manifold is well described by the semi-classical Ising vortex states, which support both a magnetic and toroidal moment along the uniaxis of the triangle. For antiferromagnetic coupling, the situation is again more interesting. For all values of $|D/J_{\text{ex}}|$ explored here (except $|D/J_{\text{ex}}| = 1$), a vanishing tunnel splitting up to $\theta < 30°$ between ground and first-excited state of the triangle is observed. These states are predominantly composed of linear combinations of the non-toroidal semi-classical Ising states $|\pm S, \pm S, \mp S\rangle$, $|\pm S, \mp S, \pm S\rangle$ and $|\mp S, \pm S, \pm S\rangle$. Similarly to the Kramers system, when these states are diagonalised on the z-component of the toroidal moment operator in Equation (1), they give rise to a ground doublet, supporting a toroidal moment, albeit with magnitude much less than an idealised, semi-classical planar arrangement of the moments $\langle \tau_z \rangle_{\text{ideal}} = 3g\mu_B R$. After $\theta \approx 30°$, the *quasi*-degeneracy is lifted with a tunnel splitting $\Delta > 10^{-2}$ cm^{-1}, and the toroidal moment drops to zero only to be recovered again for $\theta > 60°$ in the strong anisotropy limit $|D/J_{\text{ex}}| = 10$, whereby the semi-classical vortex states of the triangle become good descriptors of the *quasi*-degenerate ground state.
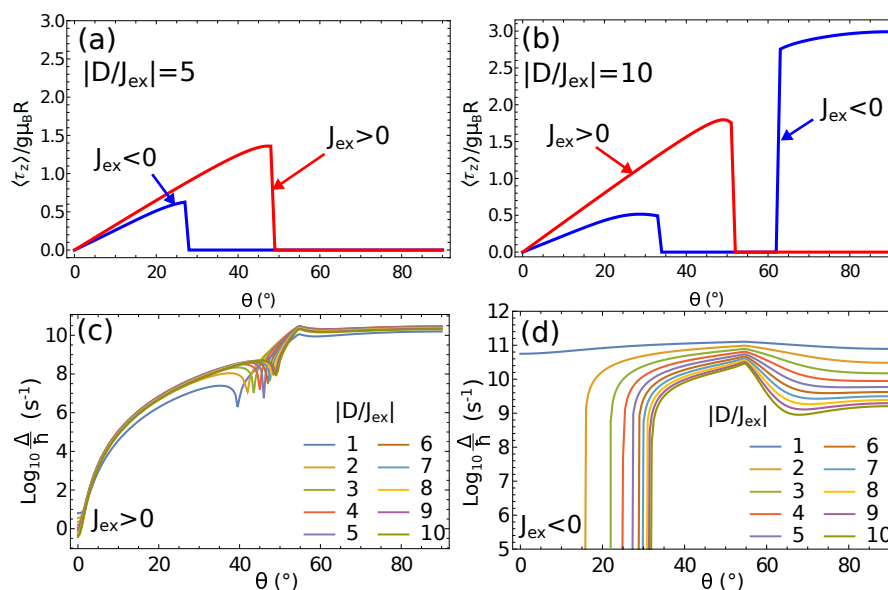
Figure 3. (**a**,**b**) Toroidal moment expectation value computed on the *quasi*-degenerate ground manifold of the triangle with ferromagnetic (red) and antiferromagnetic (blue) Heisenberg exchange coupling for (**a**) $|D/J_{ex}| = 5$ and (**b**) $|D/J_{ex}| = 10$. (**c**,**d**) Tunnelling rate of the ground-state toroidal moment as a function of canting angle θ in the molecular triangle with on-site spin $S = 1$ for a range of magnetic anisotropy strengths $|D/J_{ex}|$ and (**c**) ferromagnetic and (**d**) antiferromagnetic exchange coupling.

Figure 3c,d show the tunnelling rate $\Delta/\hbar$ of the toroidal moment, in the absence of magnetic dipole–dipole coupling, as a function of canting angle θ for a range of on-site anisotropy strengths $|D/J_{ex}|$. For both ferromagnetic and antiferromagnetic exchange coupling J_{ex}, the tunnelling rate is maximal at $\theta_0 \approx 54.7°$ where the exchange gap between the semi-classical Ising states vanishes and hence the transversal components of the linear exchange have maximal effect at mixing the semi-classical Ising ground states. For $J_{ex} < 0$, increasing the value of $|D/J_{ex}|$ leads to a diminishing of the tunnelling rate away from θ_0; however, for ferromagnetic coupling, this only occurs for $\theta \leq \theta_0$.

In Figure 4a,b, we illustrate that, for both ferromagnetic and antiferromagnetic coupling, the range of canting angles θ for which the molecular triangle displays a ground stand toroidal moment is modestly increased. This is accounted for by looking once again to the semi-classical Ising limit, where magnetic dipole–dipole coupling shifts the value of θ_0 at which the Ising exchange gap disappears. In Figure 4c,d, we show that including the fully quantum dipole–dipole coupling Hamiltonian leads to a shift of the tunnelling rate maxima to larger angles θ for $J_{ex} > 0$ and small angles θ for $J_{ex} < 0$. For the ferromagnetic case, an increase in magnetic dipole–dipole coupling also leads to an overall increase in the tunnelling rate $\Delta/\hbar$ for all canting angles θ. For strong enough dipole–dipole coupling, this can again lead to a vanishing toroidal moment for all canting angles, θ. For the realisation of robust toroidal states in quantum SMTs, magnetic dipole–dipole coupling should be maximised when antiferromagnetic exchange coupling is present; however, the situation is more complicated for ferromagnetic exchange.
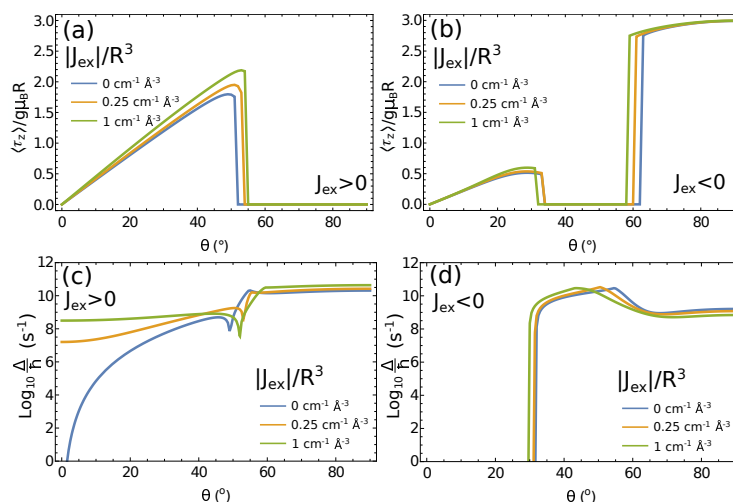
Figure 4. (**a**,**b**) Toroidal moment expectation value computed on the *quasi*-degenerate ground manifold of the triangle with (**a**) ferromagnetic and (**b**) antiferromagnetic exchange coupling for varying strengths of magnetic dipole–dipole interaction. (**c**,**d**) Tunnelling rate of the ground-state toroidal moment as a function of canting angle θ for the on-site $S = 1$ molecular triangle with a fixed ratio of $|D/J_{\text{ex}}| = 10$ and with magnetic dipole–dipole coupling included between paramagnetic sites in the ring. The tunnel splitting is shown for several dipole–dipole coupling strengths and for (**c**) ferromagnetic and (**d**) antiferromagnetic Heisenberg exchange coupling.

3. Spin Frustration in Molecular Triangles with Vanishing Magnetic Anisotropy

We now turn to the case of vanishing on-site magnetic anisotropy in the molecular triangle. This system has previously been discussed elsewhere in the context of spin electric coupling [42,55] and the realisation of ground-state toroidal moments [40], both effects based on the existence of a spin frustrated ground state when $J_{\text{ex}} < 0$. Here we recapitulate pertinent results for the triangle with a mind to extend its treatment to larger rings with intramolecular magnetic dipole–dipole coupling.

We consider a molecular triangle consisting of three isotropic $S_i = \frac{1}{2}$ spins (e.g., three $3d^9$ Cu^{2+} atoms) again arranged in an equilateral geometry in the xy-plane. The isotropic spins interact according to the following Hamiltonian:

$$H_{\text{ex}} = -J_{\text{ex}} \sum_{\langle ij \rangle} \mathbf{S}_i \cdot \mathbf{S}_j + \sum_{\langle ij \rangle} \mathbf{D}_{\text{DM}} \cdot (\mathbf{S}_i \times \mathbf{S}_j) \tag{6}$$

where $\langle ij \rangle$ denotes summation between the nearest neighbours and $\mathbf{D}_{\text{DM}} = D_{\text{DM}} \hat{\mathbf{k}}$ is the Dzyaloshinskii–Moriya interaction between neighbouring spins originating from weak spin–orbit coupling effects. The isotropic exchange coupling J_{ex} splits the eightfold degenerate Hilbert spin space of the triangle into two exchange quartets separated in energy by $\frac{3J_{\text{ex}}}{2}$. If $J_{\text{ex}} < 0$, the ground quartet is spin frustrated. The ground manifold is split further into two Kramers doublets separated in energy by $\sqrt{3}|D_{\text{DM}}|$ by the comparatively weak Dzyaloshinskii–Moriya interaction (estimated to be $D_{\text{DM}} \sim |J_{\text{ex}}|/10$) for Cu$_3$ triangles [56]).

For negative values of D_{DM}, the states comprising the ground doublet of the molecular triangle are

$$\left| M^{\text{tot}} = \frac{1}{2}, \chi = 1 \right\rangle = \frac{1}{\sqrt{3}} \left| \frac{1}{2}, \frac{1}{2}, \frac{-1}{2} \right\rangle + \frac{\epsilon_+}{\sqrt{3}} \left| \frac{1}{2}, \frac{-1}{2}, \frac{1}{2} \right\rangle + \frac{\epsilon_-}{\sqrt{3}} \left| \frac{-1}{2}, \frac{1}{2}, \frac{1}{2} \right\rangle$$

$$\left| M^{\text{tot}} = -\frac{1}{2}, \chi = -1 \right\rangle = \frac{1}{\sqrt{3}} \left| \frac{-1}{2}, \frac{-1}{2}, \frac{1}{2} \right\rangle + \frac{\epsilon_-}{\sqrt{3}} \left| \frac{-1}{2}, \frac{1}{2}, \frac{-1}{2} \right\rangle + \frac{\epsilon_+}{\sqrt{3}} \left| \frac{1}{2}, \frac{-1}{2}, \frac{-1}{2} \right\rangle \tag{7}$$

which are labelled by the total spin projection good quantum number and by the eigenvalue of the scalar chirality operator $\chi = \frac{4}{\sqrt{3}} \mathbf{S}_1 \cdot \mathbf{S}_2 \times \mathbf{S}_3$ [40,42,43], where $\epsilon_\pm = \exp(\pm 2\pi i/3)$. It

has previously been demonstrated [40,41] that the appropriate linear combinations of the $\left| M^{\text{tot}} = \pm\frac{1}{2}, \chi = \pm 1 \right\rangle$ states give rise to a ground doublet $\left| \tau_{\pm} \right\rangle = \frac{1}{\sqrt{2}} \left| M^{\text{tot}} = \frac{1}{2}, \chi = 1 \right\rangle \pm \frac{i}{\sqrt{2}} \left| M^{\text{tot}} = -\frac{1}{2}, \chi = -1 \right\rangle$, which hosts equal and opposing toroidal moments with magnitude $g\mu_B R$, pointing perpendicular to the plane of the molecular triangle. The on-site spin expectation values at each site adopt a perfectly in-plane, vortex arrangement, rotating clockwise or anticlockwise for each state.

4. Magnetic Dipole–Dipole Interactions in Extended Heisenberg Rings

As was pointed out, in a recent study of larger odd-membered Heisenberg rings [47], the antiferromagnetically coupled molecular triangle is a special case since spin frustration alone is enough to guarantee a ground manifold with toroidally polarisable states. For odd-membered rings with $N > 3$, using the Hamiltonian in Equation (6) and diagonalising the resultant exchange manifolds on the z-projection of the toroidal moment operator (Equation (1)) leads to states which support toroidal moments only in excited multiplets of the paramagnetic rings. Figure 5 illustrates this phenomenon up to nine-membered antiferromagnetically coupled rings with a weak Dzyaloshinskii–Moriya interaction.
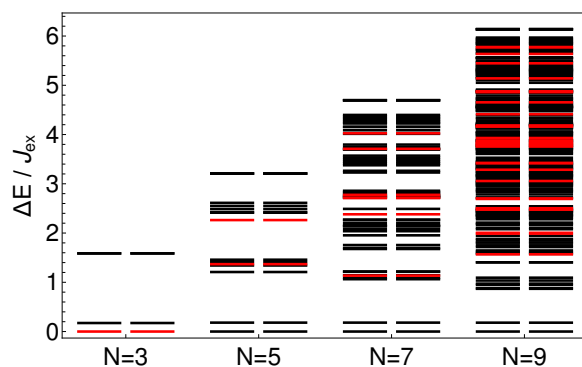

Figure 5. Energy levels for $N = 3$-, 5-, 7- and 9-membered antiferromagnetically coupled Heisenberg rings with $J_{\text{ex}} = 10D_{\text{DM}}$. Degenerate levels that support toroidal moments are labelled in red, whilst those that do not are labelled in black. Note that only for $N = 3$ are toroidal moments present in the ground state.

In [47], it was suggested that various next-nearest-neighbour isotropic exchange coupling topologies could be introduced to accentuate spin frustration and thereby stabilise toroidal moments in the ground states of $N = 5$-, 7- and 9-membered rings. The most promising coupling topology required ferromagnetic nearest neighbour and antiferromagnetic next-nearest-neighbour isotropic exchange interaction, a configuration only sparingly reported in the literature for molecular ring systems [57]. In addition, the ratio of next-nearest-neighbour to nearest neighbour exchange required toroidal states to be brought into the ground manifold, which was found to be rather stringent, such that the precise engineering of such a coupling could be challenging to achieve in practice.

Tuning intramolecular magnetic dipole–dipole interactions offers another pathway to realise ground-state toroidal moments in spin-frustrated, odd-membered Heisenberg rings, while reliably and predictably engineering odd-membered rings with precise exchange coupling topologies may be beyond the reach of current state-of-the-art synthetic chemistry, the inter-site distance of molecular Heisenberg rings (and hence the strength of magnetic dipole coupling) can more easily be controlled at the molecular scale through an appropriate choice of ligands. Since $\left[H_{\text{dip}}, S_z^{\text{tot}} \right] \neq 0$, eigenstates of the dipolar Hamiltonian (and therefore the ring Hamiltonian) can not be enumerated with the total spin projection good quantum number M^{tot} as is the case for rings with isotropic and anti-symmetric exchange coupling alone.

In Figure 6, we plot the ground-state toroidal moment as a function of $|J_{ex}|/R^3$ for 5-membered and 7-membered $S = \frac{1}{2}$ rings with ferromagnetic and antiferromagnetic exchange coupling. For rings with tightly packed metal centres, the strong intramolecular magnetic dipole–dipole coupling results in ground-state toroidal moments. As the ring size is increased the strength of dipole–dipole coupling diminishes and, at some critical radius R_*, the ground-state toroidal moment drops sharply to zero. Notably, building the magnetic dipole–dipole interaction Hamiltonian on the basis of exchange coupled eigenstates of Equation (6) revealed off-diagonal matrix elements connecting states from different exchange multiplets on the order of $\sim 1/R^3$, a similar magnitude found for the diagonal elements. This indicates that the stabilisation of the ground-state toroidal moments in larger Heisenberg rings is a non-perturbative effect of the dipole–dipole Hamiltonian. Naturally, the dipolar Hamiltonian becomes more effective at mixing states from different exchange multiplets when J_{ex} is small; thus, the critical radius for achieving ground-state toroidal moments in odd-membered rings at least up until $N = 7$ grows larger as $J_{ex} \to 0$.

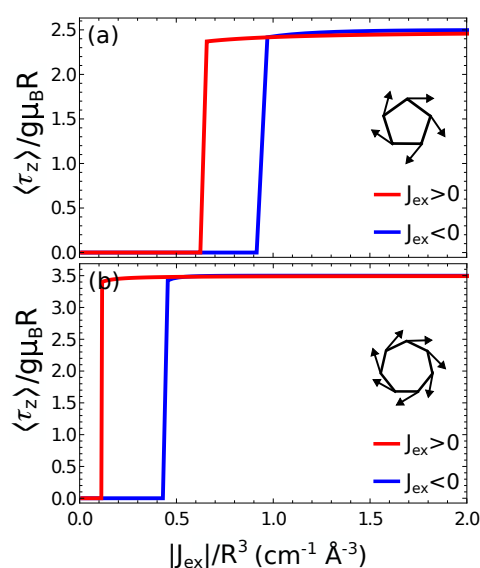**Figure 6.** Ground state expectation value of the toroidal moment operator in a five-membered (**a**) and a seven-membered (**b**) Heisenberg ring inclusive of intramolecular magnetic dipole–dipole interactions and ferromagnetic (red) or antiferromagnetic (blue) isotropic exchange coupling J_{ex}. Insets depict the expectation values of the on-site spin for one of the ring ground states below the critical circumscribed radius R_*, where a non-zero value of the toroidal moment is observed.

While engineering rings with short metal–metal bridging ligands offers a strategy to augment through-space dipole–dipole coupling, this approach has the drawback of reducing the magnitude of the ground-state toroidal moment, which is linearly proportional to the circumscribed radius of the ring, R. An alternative approach is to replace $S = \frac{1}{2}$ ions in the ring with Kramers ions that have longer spin length, e.g., Cr^{3+} with a ground $S = \frac{3}{2}$ multiplet. Accounting for isotropic exchange and magnetic dipole–dipole interactions in a Cr_5 pentagon with $|J_{ex}| = 1\ cm^{-1}$ revealed toroidal ground states that persisted in the ring up to bond lengths of 3 Å for ferromagnetic exchange and 2.4 Å for antiferromagnetic exchange.

Again, a weak Dzyaloshinskii–Moriya interaction can also stabilise the toroidal doublet of the dipole–dipole-coupled ring when $D_{DM} < 0$. Figure 7 illustrates the increase in critical radius R_* as a function of D_{DM} for rings with ferromagnetic and antiferromagnetic isotropic exchange coupling. Curiously, the Dzyaloshinskii–Moriya coupling is less effective at stabilising the toroidal ground state in antiferromagnetic-exchange-coupled rings with dipolar coupling, as opposed to the ferromagnetic case. While much rarer examples of ferromagnetically coupled Cr^{3+} rings have been reported in the literature [58], this suggests that engineering molecular wheels which satisfy some if not all of the above constraints

is a feasible approach to realising ground-state molecular toroidal moments in weakly anisotropic rings with $N > 3$.
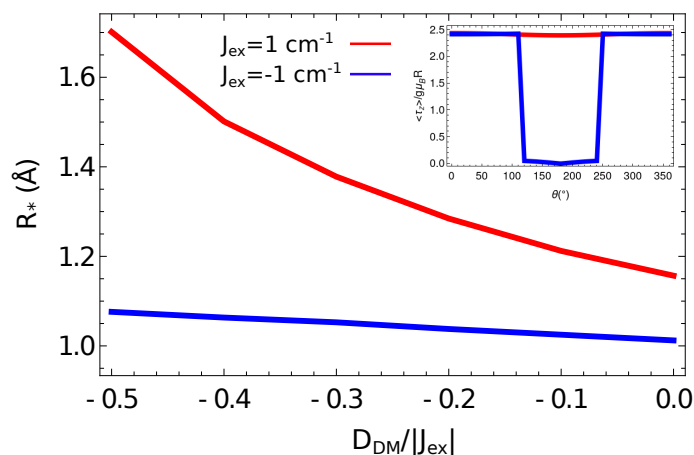

Figure 7. Critical circumscribed radius R_* at which toroidal ground states manifest in five-membered on-site $S = 1/2$ molecular wheels as function of Dzyaloshinskii–Moriya coupling strength D_{DM} in Heisenberg rings with ferromagnetic (red) and antiferromagnetic (blue) isotropic exchange coupling. Inset shows the dependence of the ground-state toroidal moment on the orientation of the $\mathbf{D}_{DM}$ vector for a 5-membered $S = 1/2$ ring with $|J_{ex}|/R = 1$ cm^{-1} Å^{-1} and $D_{DM}/|J_{ex}| = -0.1$ with ferromagnetic (red) and antiferromagnetic (blue) isotropic exchange coupling.

In this study, we have assumed a Dzyaloshinskii–Moriya vector which is uniform across all nearest neighbour bonds in the ring and which is always perpendicular to the plane of the polygon; however, this is not the most general form of the Dzyaloshinskii–Moriya interaction. In fact, a joint magnetisation and EPR study of a Cu_3 molecule found Dzyaloshinskii–Moriya vectors for the Cu-Cu pseudo-bonds with non-uniform orientations, which were related to one another by $2\pi/3$ rotations about the C_3 symmetry axis of the triangle [59]. To investigate the orientation dependence of the Dzyaloshinskii–Moriya vector on the stabilisation of ground-state toroidal moments in a five-membered ring, we parametrise the DM vector of the first bond (between paramagnetic ions 1 and 2) with the polar and azimuthal angles θ and ϕ, respectively, such that $\mathbf{D}_{DM}^{(1-2)} = D_{DM}(\cos\phi\sin\theta, \sin\phi\sin\theta, \cos\theta)$. The Dzyaloshinskii–Moriya vectors for all other bonds are generated by rotating this vector about the C_5 symmetry axis of the pentagon by the angles $\frac{2k\pi}{5}$ with $k = 1, \ldots, 4$. For both ferromagnetic and antiferromagnetic isotropic exchange coupling, and vanishing intramolecular magnetic dipole–dipole coupling, varying the orientations of the Dzyaloshinskii–Moriya vectors may only weakly induce a ground-state toroidal moment whose magnitude is <5 % (for all θ and ϕ) of the maximal theoretical value, $\frac{5}{2}\mu_B gR$. In the inset of Figure 7, we investigate the effect of different Dzyaloshinskii–Moriya vector orientations on the ground-state toroidal moment of the molecular pentagon with strong intramolecular magnetic dipole–dipole coupling, while the ground-state toroidal moment in the ferromagnetically coupled pentagon appears approximately invariant to different Dzyaloshinskii–Moriya vector orientations, we observe a precipitous drop in the toroidal moment expectation value of the antiferromagnetic ring when $\theta = \frac{2\pi}{3}$. This behaviour is reproduced for all choices of ϕ. It is hence noteworthy that, if possible, molecular wheels with vanishing on-site magnetic anisotropy should be engineered with Dzyaloshinskii–Moriya vectors, oriented as perpendicular to the ring as possible to support ground-state toroidal moments.

5. Discussion and Conclusions

For the development of novel SMT-based quantum information technologies employing toroidal qubits, a fully quantum description of SMTs is imperative. Quantum effects have been shown here and elsewhere [19] to disrupt the formation of toroidal ground states

in SMTs by introducing tunnelling mechanisms between the semi-classical magnetic vortex ground states of the ring. Here we have investigated the role of intramolecular magnetic dipole–dipole coupling in quantum SMTs, demonstrating, for the prototypical triangular SMT motif, that dipole–dipole coupling extends the range of magnetic axis canting angles, for which one may observe toroidal ground states in both ferromagnetic and antiferromagnetically coupled triangles with strong on-site anisotropy. In the weak anisotropy limit, despite the fact that antiferromagnetically coupled $N > 3$ Heisenberg rings do not usually support ground-state toroidal moments, we have demonstrated that, by utilising the bond-length-sensitive, intramolecularly magnetic dipole–dipole interaction, these toroidal states can be stabilised at some critical radius, R_*. In addition, we demonstrated that the critical radius, R_*, required to observe toroidal ground states in the molecular pentagon, may be augmented by increasing on-site spin length and also by increasing the magnitude of Dzyaloshinskii–Moriya coupling $|D_{DM}|$. Finally, we commented on the orientation dependence of the Dzyaloshinskii–Moriya vectors in stabilising a ground-state toroidal moment in molecular wheels.

Author Contributions: K.H. and A.S. have contributed, in all aspects, equally to this manuscript. All authors have read and agreed to the published version of the manuscript.

Institutional Review Board Statement: Not applicable.

Informed Consent Statement: Not applicable.

Data Availability Statement: Not applicable.

Conflicts of Interest: The authors declare no conflict of interest.

Abbreviations

The following abbreviations are used in this manuscript:

SMM	Single-molecule magnet
SMT	Single-molecule toroic

References

1. Zel'Dovich, I.B. Electromagnetic interaction with parity violation. *Sov. Phys. JETP* **1958**, *6*, 1184–1186.
2. Wood, C.; Bennett, S.; Cho, D.; Masterson, B.; Roberts, J.; Tanner, C.; Wieman, C.E. Measurement of parity nonconservation and an anapole moment in cesium. *Science* **1997**, *275*, 1759–1763. [CrossRef] [PubMed]
3. Marinov, K.; Boardman, A.; Fedotov, V.; Zheludev, N. Toroidal metamaterial. *New J. Phys.* **2007**, *9*, 324. [CrossRef]
4. Wätzel, J.; Berakdar, J. Open-Circuit Ultrafast Generation of Nanoscopic Toroidal Moments: The Swift Phase Generator. *Adv. Quantum Technol.* **2019**, *2*, 1970011. [CrossRef]
5. Ho, C.M.; Scherrer, R.J. Anapole dark matter. *Phys. Lett. B* **2013**, *722*, 341–346. [CrossRef]
6. Lewis, R.R. Anapole moment of a diatomic polar molecule. *Phys. Rev. A* **1994**, *49*, 3376. [CrossRef] [PubMed]
7. Ceulemans, A.; Chibotaru, L.; Fowler, P. Molecular anapole moments. *Phys. Rev. Lett.* **1998**, *80*, 1861. [CrossRef]
8. Pelloni, S.; Faglioni, F.; Soncini, A.; Ligabue, A.; Lazzeretti, P. Magnetic response of dithiin molecules: Is there anti-aromaticity in nature? *Chem. Phys. Lett.* **2003**, *375*, 583–590. [CrossRef]
9. Faglioni, F.; Ligabue, A.; Pelloni, S.; Soncini, A.; Lazzeretti, P. Molecular response to a time-independent non-uniform magnetic-field. *Chem. Phys.* **2004**, *304*, 289–299. [CrossRef]
10. Borschevsky, A.; Iliaš, M.; Dzuba, V.; Flambaum, V.; Schwerdtfeger, P. Relativistic study of nuclear-anapole-moment effects in diatomic molecules. *Phys. Rev. A* **2013**, *88*, 022125. [CrossRef]
11. Pelloni, S.; Faglioni, F.; Zanasi, R.; Lazzeretti, P. Topology of magnetic-field-induced current-density field in diatropic monocyclic molecules. *Phys. Rev. A* **2006**, *74*, 012506. [CrossRef]
12. Carion, R.; Champagne, B.; Monaco, G.; Zanasi, R.; Pelloni, S.; Lazzeretti, P. Ring current model and anisotropic magnetic response of cyclopropane. *J. Chem. Theory Comput.* **2010**, *6*, 2002–2018. [CrossRef] [PubMed]
13. Monaco, G.; Summa, F.F.; Zanasi, R. Program Package for the Calculation of Origin-Independent Electron Current Density and Derived Magnetic Properties in Molecular Systems. *J. Chem. Inf. Model.* **2020**, *61*, 270–283. [CrossRef] [PubMed]

14. Summa, F.F.; Monaco, G.; Lazzeretti, P.; Zanasi, R. Assessment of the performance of DFT functionals in the fulfillment of off-diagonal hypervirial relationships. *Phys. Chem. Chem. Phys.* **2021**, *23*, 15268–15274. [CrossRef] [PubMed]

15. Pelloni, S.; Lazzeretti, P.; Monaco, G.; Zanasi, R. Magnetic-field induced electronic anapoles in small molecules. *Rend. Lincei* **2011**, *22*, 105–112. [CrossRef]

16. Summa, F.F.; Monaco, G.; Zanasi, R.; Lazzeretti, P. Dynamic Toroidisability as Ubiquitous Property of Atoms and Molecules in Optical Electric Fields. *J. Chem. Phys.* **2022**, *156*, 054106. [CrossRef]

17. Dubovik, V.; Tugushev, V. Toroid moments in electrodynamics and solid-state physics. *Phys. Rep.* **1990**, *187*, 145–202. [CrossRef]

18. Spaldin, N.A.; Fiebig, M.; Mostovoy, M. The toroidal moment in condensed-matter physics and its relation to the magnetoelectric effect. *J. Phys. Condens. Matter* **2008**, *20*, 434203. [CrossRef]

19. Soncini, A.; Chibotaru, L.F. Toroidal magnetic states in molecular wheels: Interplay between isotropic exchange interactions and local magnetic anisotropy. *Phys. Rev. B* **2008**, *77*, 220406. [CrossRef]

20. Tang, J.; Hewitt, I.; Madhu, N.; Chastanet, G.; Wernsdorfer, W.; Anson, C.E.; Benelli, C.; Sessoli, R.; Powell, A.K. Dysprosium triangles showing single-molecule magnet behavior of thermally excited spin states. *Angew. Chem.* **2006**, *118*, 1761–1765. [CrossRef]

21. Chibotaru, L.F.; Ungur, L.; Soncini, A. The origin of nonmagnetic Kramers doublets in the ground state of dysprosium triangles: Evidence for a toroidal magnetic moment. *Angew. Chem.* **2008**, *120*, 4194–4197. [CrossRef]

22. Wang, Y.X.; Shi, W.; Li, H.; Song, Y.; Fang, L.; Lan, Y.; Powell, A.K.; Wernsdorfer, W.; Ungur, L.; Chibotaru, L.F.; et al. A single-molecule magnet assembly exhibiting a dielectric transition at 470 K. *Chem. Sci.* **2012**, *3*, 3366–3370. [CrossRef]

23. Xue, S.; Chen, X.H.; Zhao, L.; Guo, Y.N.; Tang, J. Two bulky-decorated triangular dysprosium aggregates conserving vortex-spin structure. *Inorg. Chem.* **2012**, *51*, 13264–13270. [CrossRef] [PubMed]

24. Zhu, Z.H.; Ma, X.F.; Wang, H.L.; Zou, H.H.; Mo, K.Q.; Zhang, Y.Q.; Yang, Q.Z.; Li, B.; Liang, F.P. A triangular Dy 3 single-molecule toroic with high inversion energy barrier: Magnetic properties and multiple-step assembly mechanism. *Inorg. Chem. Front.* **2018**, *5*, 3155–3162. [CrossRef]

25. Langley, S.K.; Vignesh, K.R.; Gupta, T.; Gartshore, C.J.; Rajaraman, G.; Forsyth, C.M.; Murray, K.S. New examples of triangular terbium (III) and holmium (III) and hexagonal dysprosium (III) single molecule toroics. *Dalton Trans.* **2019**, *48*, 15657–15667. [CrossRef]

26. Das, C.; Vaidya, S.; Gupta, T.; Frost, J.M.; Righi, M.; Brechin, E.K.; Affronte, M.; Rajaraman, G.; Shanmugam, M. Single-molecule magnetism, enhanced magnetocaloric effect, and toroidal magnetic moments in a family of Ln4 squares. *Chemistry* **2015**, *21*, 15639–15650. [CrossRef]

27. Gusev, A.; Herchel, R.; Nemec, I.; Shul'gin, V.; Eremenko, I.L.; Lyssenko, K.; Linert, W.; Travnicek, Z. Tetranuclear lanthanide complexes containing a hydrazone-type ligand. Dysprosium [2 × 2] gridlike single-molecule magnet and toroic. *Inorg. Chem.* **2016**, *55*, 12470–12476. [CrossRef]

28. Fernandez Garcia, G.; Guettas, D.; Montigaud, V.; Larini, P.; Sessoli, R.; Totti, F.; Cador, O.; Pilet, G.; Le Guennic, B. A Dy4 Cubane: A New Member in the Single-Molecule Toroics Family. *Angew. Chem.* **2018**, *130*, 17335–17339. [CrossRef]

29. Ungur, L.; Langley, S.K.; Hooper, T.N.; Moubaraki, B.; Brechin, E.K.; Murray, K.S.; Chibotaru, L.F. Net toroidal magnetic moment in the ground state of a {Dy6}-triethanolamine ring. *J. Am. Chem. Soc.* **2012**, *134*, 18554–18557. [CrossRef]

30. Holmberg, R.J.; Kuo, C.J.; Gabidullin, B.; Wang, C.W.; Clérac, R.; Murugesu, M.; Lin, P.H. A propeller-shaped μ 4-carbonate hexanuclear dysprosium complex with a high energetic barrier to magnetisation relaxation. *Dalton Trans.* **2016**, *45*, 16769–16773. [CrossRef]

31. Lu, J.; Montigaud, V.; Cador, O.; Wu, J.; Zhao, L.; Li, X.L.; Guo, M.; Le Guennic, B.; Tang, J. Lanthanide (III) hexanuclear circular helicates: Slow magnetic relaxation, toroidal arrangement of magnetic moments, and magnetocaloric effects. *Inorg. Chem.* **2019**, *58*, 11903–11911. [CrossRef] [PubMed]

32. Novitchi, G.; Pilet, G.; Ungur, L.; Moshchalkov, V.V.; Wernsdorfer, W.; Chibotaru, L.F.; Luneau, D.; Powell, A.K. Heterometallic Cu II/Dy III 1D chiral polymers: Chirogenesis and exchange coupling of toroidal moments in trinuclear Dy 3 single molecule magnets. *Chem. Sci.* **2012**, *3*, 1169–1176. [CrossRef]

33. Vignesh, K.R.; Soncini, A.; Langley, S.K.; Wernsdorfer, W.; Murray, K.S.; Rajaraman, G. Ferrotoroidic ground state in a heterometallic {Cr III Dy III 6} complex displaying slow magnetic relaxation. *Nat. Commun.* **2017**, *8*, 1023. [CrossRef] [PubMed]

34. Vignesh, K.R.; Langley, S.K.; Swain, A.; Moubaraki, B.; Damjanović, M.; Wernsdorfer, W.; Rajaraman, G.; Murray, K.S. Slow Magnetic Relaxation and Single-Molecule Toroidal Behaviour in a Family of Heptanuclear {CrIIILnIII6}(Ln= Tb, Ho, Er) Complexes. *Angew. Chem.* **2018**, *130*, 787–792. [CrossRef]

35. Ashtree, J.M.; Borilović, I.; Vignesh, K.R.; Swain, A.; Hamilton, S.H.; Whyatt, Y.L.; Benjamin, S.L.; Phonsri, W.; Forsyth, C.M.; Wernsdorfer, W.; et al. Tuning the Ferrotoroidic Coupling and Magnetic Hysteresis in Double-Triangle Complexes {Dy3MIIIDy3} via the MIII-linker. *Eur. J. Inorg. Chem.* **2021**, *2021*, 435–444. [CrossRef]

36. Lin, S.Y.; Wernsdorfer, W.; Ungur, L.; Powell, A.K.; Guo, Y.N.; Tang, J.; Zhao, L.; Chibotaru, L.F.; Zhang, H.J. Coupling Dy3 triangles to maximize the toroidal moment. *Angew. Chem. Int. Ed.* **2012**, *51*, 12767–12771. [CrossRef]

37. Li, X.L.; Wu, J.; Tang, J.; Le Guennic, B.; Shi, W.; Cheng, P. A planar triangular Dy 3+ Dy 3 single-molecule magnet with a toroidal magnetic moment. *Chem. Commun.* **2016**, *52*, 9570–9573. [CrossRef]

38. Lin, S.Y.; Wu, J.; Xu, Z. The effect of additional methyl on the magnetic relaxation and toroidal moment of Dy 6 complex. *RSC Adv.* **2017**, *7*, 47520–47526. [CrossRef]

39. Nielsen, M.A.; Chuang, I. Quantum computation and quantum information. In *Mathematical Structures in Computer Science*; United States of America by Cambridge University Press: New York, NY, USA, 2002; Volume 17, p. 1115.
40. Crabtree, J.M.; Soncini, A. Toroidal quantum states in molecular spin-frustrated triangular nanomagnets with weak spin–orbit coupling: Applications to molecular spintronics. *Phys. Rev. B* **2018**, *98*, 094417. [CrossRef]
41. Rao, S.; Ashtree, J.; Soncini, A. Toroidal moment in a family of spin-frustrated heterometallic triangular nanomagnets without spin–orbit coupling: Applications in a molecular spintronics device. *Phys. B Condens. Matter* **2020**, *592*, 412237. [CrossRef]
42. Trif, M.; Troiani, F.; Stepanenko, D.; Loss, D. Spin-electric coupling in molecular magnets. *Phys. Rev. Lett.* **2008**, *101*, 217201. [CrossRef] [PubMed]
43. Trif, M.; Troiani, F.; Stepanenko, D.; Loss, D. Spin electric effects in molecular antiferromagnets. *Phys. Rev. B* **2010**, *82*, 045429. [CrossRef]
44. Plokhov, D.; Zvezdin, A.; Popov, A. Macroscopic quantum dynamics of toroidal moment in Ising-type rare-earth clusters. *Phys. Rev. B* **2011**, *83*, 184415. [CrossRef]
45. Pavlyuk, Y. Toroidal spin states in molecular magnets. *Phys. Rev. B* **2020**, *101*, 144408. [CrossRef]
46. Liu, J.; Mrozek, J.; Myers, W.K.; Timco, G.A.; Winpenny, R.E.; Kintzel, B.; Plass, W.; Ardavan, A. Electric field control of spins in molecular magnets. *Phys. Rev. Lett.* **2019**, *122*, 037202. [CrossRef]
47. Rao, S.V. Development and Application of Theoretical Models for Molecular Magnetism. Ph.D. Thesis, University of Melbourne, Melbourne, VIC, Australia, 2019.
48. Abragam, A.; Bleaney, B. *Electron Paramagnetic Resonance of Transition Ions*; OUP Oxford: Oxford, UK, 2012.
49. Noodleman, L. Valence bond description of antiferromagnetic coupling in transition metal dimers. *J. Chem. Phys.* **1981**, *74*, 5737–5743. [CrossRef]
50. Bellini, V.; Olivieri, A.; Manghi, F. Density-functional study of the Cr 8 antiferromagnetic ring. *Phys. Rev. B* **2006**, *73*, 184431. [CrossRef]
51. Vélez, E.; Alberola, A.; Polo, V. A density functional theory study of the magnetic exchange coupling in dinuclear manganese (II) inverse crown structures. *J. Phys. Chem. A* **2009**, *113*, 14008–14013. [CrossRef]
52. Craig, D.P.; Thirunamachandran, T. *Molecular Quantum Electrodynamics: An Introduction to Radiation-Molecule Interactions*; Courier Corporation: Chelmsford, MA, USA, 1998.
53. Luzon, J.; Bernot, K.; Hewitt, I.J.; Anson, C.E.; Powell, A.K.; Sessoli, R. Spin chirality in a molecular dysprosium triangle: The archetype of the noncollinear Ising model. *Phys. Rev. Lett.* **2008**, *100*, 247205. [CrossRef]
54. Rousset, E.; Piccardo, M.; Boulon, M.E.; Gable, R.W.; Soncini, A.; Sorace, L.; Boskovic, C. Slow magnetic relaxation in lanthanoid crown ether complexes: Interplay of Raman and anomalous phonon bottleneck processes. *Chem. Eur. J.* **2018**, *24*, 14768–14785. [CrossRef] [PubMed]
55. Islam, M.F.; Nossa, J.F.; Canali, C.M.; Pederson, M. First-principles study of spin-electric coupling in a {Cu_ {3}} single molecular magnet. *Phys. Rev. B* **2010**, *82*, 155446. [CrossRef]
56. Ferrer, S.; Lloret, F.; Pardo, E.; Clemente-Juan, J.M.; Liu-Gonzalez, M.; Garcia-Granda, S. Antisymmetric exchange in triangular tricopper (II) complexes: Correlation among structural, magnetic, and electron paramagnetic resonance parameters. *Inorg. Chem.* **2012**, *51*, 985–1001. [CrossRef] [PubMed]
57. Baniodeh, A.; Magnani, N.; Lan, Y.; Buth, G.; Anson, C.E.; Richter, J.; Affronte, M.; Schnack, J.; Powell, A.K. High spin cycles: Topping the spin record for a single molecule verging on quantum criticality. *NPJ Quantum Mater.* **2018**, *3*, 10. [CrossRef]
58. Fu, Z.; Qin, L.; Sun, K.; Hao, L.; Zheng, Y.Z.; Lohstroh, W.; Günther, G.; Russina, M.; Liu, Y.; Xiao, Y.; et al. Low-temperature spin dynamics of ferromagnetic molecular ring {Cr8Y8}. *NPJ Quantum Mater.* **2020**, *5*, 32. [CrossRef]
59. Choi, K.Y.; Matsuda, Y.H.; Nojiri, H.; Kortz, U.; Hussain, F.; Stowe, A.C.; Ramsey, C.; Dalal, N.S. Observation of a Half Step Magnetization in the {Cu3}-Type Triangular Spin Ring. *Phys. Rev. Lett.* **2006**, *96*, 107202. [CrossRef]